

## §21. Ray Tracing of Ion Bernstein Wave Using Folded Waveguide Antenna

Torii, Y. (Nagoya Univ.), Kumazawa, R.

On LHD, the minority heating using fast wave was performed and demonstrated that ICRF heating was one of the effective heating methods also in a helical device. In the ICRF heating, the fast wave heating contributed to achieve the high temperature and the high density plasma.

On the other hand, several interesting experimental results of slow wave experiments were reported. On the LHD, plasma production experiment using a folded waveguide antenna was carried out; plasma was produced. In this experiment, the folded waveguide antenna launched shear Alfvén wave<sup>1)</sup>.

Interesting experimental results of ion Bernstein wave (IBW) also were reported. On the JIPP TII-U, reduction of impurities, and peaking of electron density, electron temperature and ion temperature were observed by IBW heating<sup>2)</sup>. It may be expected that confinement improvement occurs also on the LHD. For efficient experiment execution, the wave propagation and damping mechanism were examined with ray tracing method<sup>3)</sup>.

In this research, following heating scenarios are investigated. In helium plasma, ion Bernstein wave is launched by a slow wave antenna which locates the weaker magnetic field side of the LHD. The magnetic field strength is employed in the third harmonics of helium cyclotron resonance near the antenna. The wave propagates into the central region and is damped near the second cyclotron resonance layer.

The ray trajectory is calculated using following equations;

$$\begin{cases} \frac{d\mathbf{r}}{dt} = -\frac{\partial D}{\partial \mathbf{k}} \bigg/ \frac{\partial D}{\partial \omega} \\ \frac{d\mathbf{k}}{dt} = \frac{\partial D}{\partial \mathbf{r}} \bigg/ \frac{\partial D}{\partial \omega} \end{cases}$$

where,  $\mathbf{r}$ ,  $\mathbf{k}$ ,  $D$ , and  $\omega$  are a position vector, a wavenumber vector, a determinant of the dispersion relation, and applied frequency, respectively.

The ray tracing results are shown in Fig.1 for two magnetic field strength, *i.e.*  $B_{ax} = 2.38, 2.67\text{T}$ . In this calculation,  $f = 37.43\text{MHz}$ ,  $k_{\parallel} = 3.0\text{m}^{-1}$  are employed. The rays oscillate along the magnetic line of force and gradually approach the plasma core. Figure 2 shows power deposition profiles in the two different magnetic field strength. All wave energies are absorbed by electrons in both cases. It is noted that, even near the ion cyclotron resonance layer, wave damping by electrons is dominant, since the parallel wavenumber become large.

The ray tracing calculation is performed in various conditions. Waves go into the central region and the wave energies are absorbed mainly by electrons in any case. By changing the shapes of temperature and density

profiles, the differences of the wave propagation and the deposition profile are examined. The trajectories and deposition profiles vary little.

The dependence on temperature is examined. In the higher temperature, damping occurs in the broader region, since the electron thermal velocity approaches the phase velocity.

The parallel wavenumber affect the ray trajectory. The calculations are performed by changing the initial value of the parallel wavenumber. In the case of the small parallel wavenumber, the ray oscillates in the small swing width along the magnetic field line and proceed into central region.

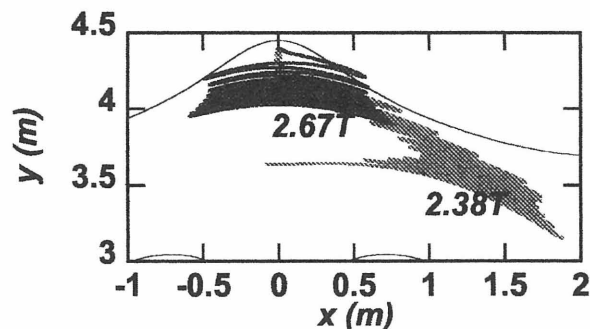


Figure 1: The calculated ray trajectories of two cases of the magnetic field strength.

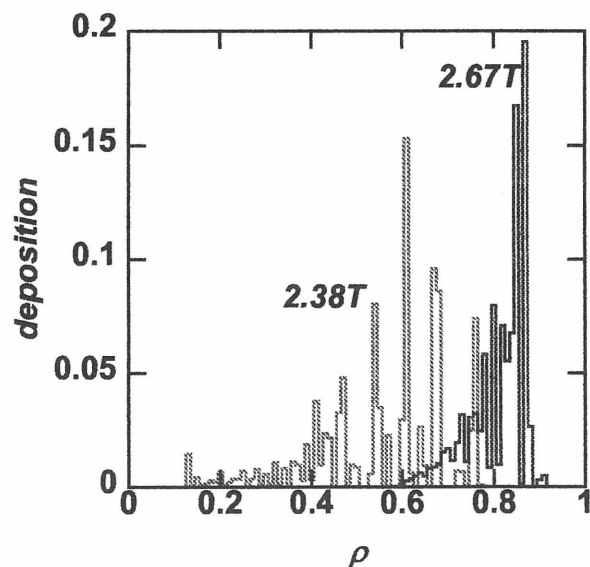


Figure 2: Power deposition profile by the ray tracing calculation. All wave energy are absorbed by electron in both case.

### Reference

- 1) Y. Torii, et al., Nuclear Fusion, **42** (2002) 679
- 2) T. Seki, et al., Nuclear Fusion, **32** (1992) 2189
- 3) B. D. McVey, Nuclear Fusion, **19** (1979) 461